Simultaneous measurement of electronic and vibrational dynamics to clarify a geometrical relaxation process in a conjugated polymer

Juan Du,[1,2] Zhuan Wang,[1,2] Wei Feng,[3] Katsumi Yoshino,[3] and Takayoshi Kobayashi[1,2,4,5,*]

[1]*Department of Applied Physics and Chemistry and Institute for Laser Science, The University of Electro-communications, 1-5-1 Chofugaoka, Chofu, Tokyo 182-8585, Japan*

[2]*ICORP, JST, Ultrashort Pulse Laser Project, 4-1-8 Honcho, Kawaguchi, Saitama 332-0012, Japan*

[3]*Center for Advanced Science and Innovation, Osaka University, Yamada-Oka, Suita, Osaka 565-0871, Japan*

[4]*Department of Electrophysics, National Chiao Tung University, 1001 Ta Hsueh Road, Hsin-Chu 3005, Taiwan*

[5]*Institute of Laser Engineering, Osaka University, 2-6 Yamada-Oka, Suita, Osaka 565-0971, Japan*

(Received 5 December 2007; revised manuscript received 9 April 2008; published 15 May 2008)

The real-time vibrational spectroscopy was utilized to obtain both electronic and vibrational dynamics in a conjugated polymer under the same excitation and probing condition by using the same sample and observing at the same time. Most of the conjugated polymers are in an amorphous phase, in which there is a relatively broad distribution of chain length, conjugation length, and degree of interaction strength between neighboring chains. Because of the varieties, a simultaneous measurement of electronic and vibrational dynamics in a broad spectral range is considered to be most powerful to study such systems as conjugated polymers. In the present paper, we performed this type of experiment of the simultaneous probing of electronic and vibrational relaxations at 128 wavelengths. The sample studied here is an amino-moiety-containing conjugated polymer, poly{[3-hexylthiophene-2,5-diyl]-[*p*-dimethylaminobenzylidenequinoidmethene]} (PHTDMABQ), whose monomer is a derivative of a thiophene oligomer. The light source is a few-cycle pulse laser with an ultimate time resolution of 0.2 fs in the visible and near IR ranges. The data containing both electronic relaxation and vibrational dynamics were analyzed to obtain a more reliable relaxation mechanism of the excitations than a combination of individual studies of electronic and vibrational relaxations. By utilizing the ultrafast pump-probe spectroscopic system, we could identify the exciton state with a π-electron delocalized in benzilidene ring. In the polymer PHTDMABQ, the geometrical relaxation from the free exciton to the exciton polaron takes place in 60–100 fs. This time is close to that observed in several polydiacetylenes previously reported. The C-C single bond stretching frequencies of the free exciton and exciton polaron are about 1300 and 1350 cm^{-1}. The coherent molecular vibration after the geometrical relaxation is considered to be a kind of reaction induced coherence. This coherent vibration decays with the time constant of about 450 fs.

DOI: 10.1103/PhysRevB.77.195205 PACS number(s): 78.47.J−, 42.65.Re

I. INTRODUCTION

The coexistence of semiconductivity, plasticity, and chemical design flexibility makes conjugated polymers remarkable materials, since these properties are expected to be very useful for electro-optical applications in various circumstances.[1–4] The efficiency and the dynamics of elementary excitations in this class of materials were the subjects of intense research activities.[5–8] These materials, including conjugated polymers, have recently been a focus of research on new nonlinear optical (NLO) materials because of their often ultrafast and large third-order NLO susceptibility, which is expected to be useful in devices such as all-optical switches.

There are two groups of conjugated polymers classified in terms of the degeneracy of their electronic ground state. They are those with the degenerate and nondegenerate ground states. The former has nonlinear excitations of solitons and charged polarons as in *trans*-polyacetylene.[6] The latter has a nonlinear excitation of neutral bipolarons (sometimes called exciton polarons or self-trapped excitons) as in *cis*-polyacetylene and polydiacetylene.[5,6,9] The ultrafast geometrical relaxation takes place just after photoexcitation by any small but finite vibronic coupling in such a one-dimensional chain because of the general feature of instability of such excitations in a low-dimensional system.[6,9,10] Because of an ultrafast drastic spectral change associated with the electronic stabilization induced by the spontaneous relaxation, they exhibit both absorptive and dispersive ultrafast optical nonlinearities.[9] Since this ultrafast relaxation takes place via vibronic coupling, it is of vital importance to study the mechanism and dynamics of vibronic coupling to clarify the ultrafast nonlinear optical dynamics.

Most of the morphology of conjugated polymer systems is amorphous except for a few polymers, which can form single crystals such as several polydiacetylene derivatives.[9,11–16] Therefore, such amorphous polymers have highly inhomogeneous electronic states due to the distributed degrees of polymerization and conjugation lengths. They are also expected to be inhomogeneous in their vibrational properties. Furthermore, they have various degrees of interaction strength and different types of interactions such as main chain–main chain, main chain–side group, and side group–side group interactions. Therefore, the relaxation dynamics of electronic states coupled to vibrational levels, which results in electronic relaxation, is considered to be very complicated because of the various contributions of the inhomogeneous system to the relaxation mechanisms depending on the properties of electronic states and vibrational levels. In order to disentangle the inhomogeneity of decay dynamics, it is

needed to study both electronic and vibrational dynamics for the same system under the same condition. It is highly desired that the measurements of the two dynamics is to be made at the same time or, at least, by using the same light source and detection system. In general, the electronic relaxation dynamics is studied by conventional pump-probe experiments, degenerate four-wave mixing, and several other methods such as pulsed light pump-photoacoustic probe. Vibrational relaxation has been mainly studied by time-resolved Raman scattering spectroscopy or time-resolved infrared (IR) absorption spectroscopy. In these experiments, most frequently, an ultraviolet or visible pump pulse generates excited states or starts a photochemical reaction, and a probe pulse detects the change in the Raman or IR spectrum.[17–19]

The methodology used in the present study is the femtosecond pump-probe real-time spectroscopy technique. This was applied to investigate both the vibrational and electronic dynamics in a molecule. Compared with conventional vibrational spectroscopies, such as infrared absorption and Raman scattering techniques, this method has the following five advantages: (1) resonance Raman signals are very frequently overwhelmed by the fluorescence signal, especially in the case of highly fluorescent molecules. In contrast, in the case of real-time vibrational spectroscopy, the effect of spontaneous fluorescence can be almost eliminated because of a much more intense and spatially coherent probe beam than spontaneous fluorescence. (2) The low frequency modes can easily be studied by pump probe as long as a few quanta of the modes can be covered within the width of the laser spectrum with nearly constant phase; however, it is difficult to detected by using a Raman scattering method due to intense Rayleigh scattering of the excitation beam. For example, modes with lower frequency than 200 cm^{-1} are difficult to detect by the conventional Raman spectroscopy, but it is easy to measure by the real-time spectroscopy. (3) As a pure time domain technique, the pump-probe method enables a direct observation of vibronic dynamics including time-dependent instantaneous frequencies. In the case of conventional time-resolved vibrational spectroscopy, a time-dependent frequency can be detected with a much longer time step than the pulse duration. Therefore, the change to be followed is in the time step of a subpicosecond regime. Hence, it is difficult to detect a change in this vibrational frequency within an oscillation period. On the other hand, in the case of real-time spectroscopy, using the time step of 0.1 or 0.2 fs (as used in our group), a very small change in frequency shifting can be detected nearly continuously in real-time domain. In the case of time-resolved Raman spectroscopy, Raman spectra at delay times are taken, but the difference between the delay times cannot be well controlled in a sub-1-fs time range. Therefore, molecular structural change information like that in the transition state cannot be detected. (4) The real-time spectroscopy can provide information on vibrational phase, which can never be obtained with conventional Raman or infrared spectroscopy. (5) By using real-time spectroscopy, we can simultaneously investigate the dynamics of vibrational modes coupled to the electronic transition in relation to the decay dynamics of the electronic excited states under exactly the same experimental conditions.

Recently, an IR pump–IR probe experiment also became popular in studying vibrational relaxation processes.[17–19]

In this paper, investigation has been made on both electronic and vibrational relaxation processes in an amino-moiety-containing conjugated polymer, poly{[3-hexylthiophene-2,5-diyl] - [*p*-dimethylaminobenzylidenequinoidmethene]} (PHTDMABQ), by real-time vibrational spectroscopy with a few-cycle pulse laser that has an ultimate time resolution of 0.2 fs in the visible and near IR ranges. We analyzed the data containing both electronic relaxation and vibrational dynamics to obtain a more reliable relaxation mechanism of the excitations than a combination of individual studies of electronic and vibrational relaxations.

II. EXPERIMENT

A. Ultrashort pulse laser system

Both pump and probe pulses were from a noncollinear optical parametric amplifier (NOPA) seeded by a white-light continuum.[20–25] The pulse duration of the NOPA output was compressed with a system composed of a pair of Brewster angle prisms that have an apex angle of 68° and chirp mirrors (Layertec). A typical visible near IR pulse with a pulse duration of 6.3 fs (Δt=6.3 fs) covered the spectral range extending from 515 to 716 nm ($\Delta \nu$=1796 cm^{-1}), with time-bandwidth product of $\Delta \nu \Delta t$=0.34, which indicates that the pulses were nearly Fourier-transform (FT) limited. The pulse energies of the pump and probe were typically about 50 and 6 nJ, respectively. The pump source of this NOPA system is a commercially supplied regenerative amplifier (Spectra Physics, Spitfire), whose central wavelength, pulse duration, repetition rate, and average output power were 800 nm, 50 fs, 5 kHz, and 650 mW, respectively.

In the present experiment, we applied the combination of polychromator and multichannel lock-in amplifier to detect the pump-probe signal. The reference and probe pulses were dispersed by the polychromator (300 groove/mm, 500 nm blazed) and simultaneously guided to the photodetector by a 128-channel bundle fiber. The spectral resolution of the total system, which is composed of the monochromator, bundle fiber, and photodetector, was about 1.5 nm. The wavelength dependent difference absorbance of the probe was measured for 128 wavelengths at pump-probe delay times from −200 to 1800 fs, with a delay time step of 0.2 fs. All of the experiments were performed at a constant temperature (293 K).

B. Materials

The sample studied here is a PHTDMABQ, whose monomer is a derivative of a thiophene oligomer. The stationary absorption and the fluorescence spectra of PHTDMABQ were measured with an absorption spectrometer (Shimadzu, UV-3101PC) and a fluorophotometer (Hitachi, F-4500), respectively. PHTDMABQ was dissolved in methanol and cast on a quartz substrate for the measurement of stationary and time-resolved spectra.

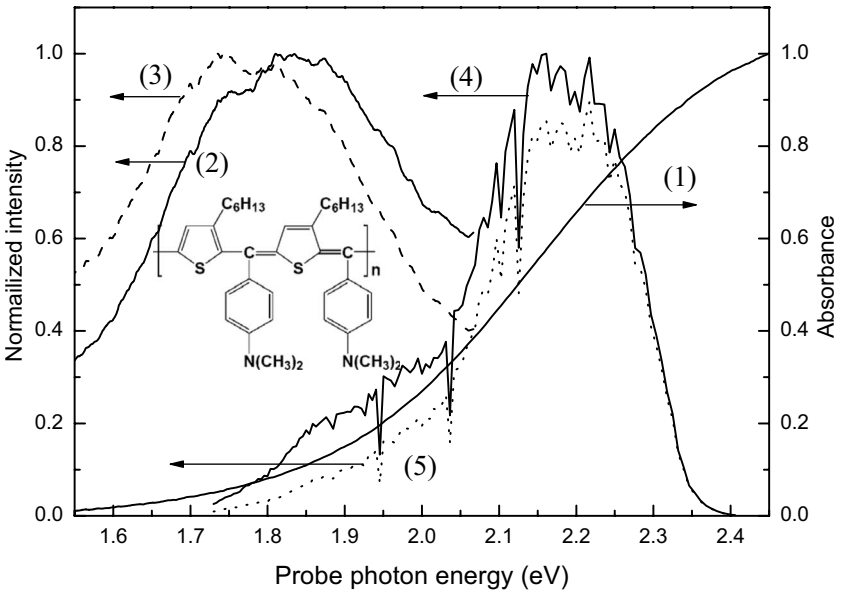

FIG. 1. The absorption spectrum (1), fluorescence spectrum (2), and stimulated emission spectrum (3) of PHTDMABQ cast film on a quartz substrate, the NOPA laser spectrum (4), and the absorbed laser photon energy distribution of spectrum by PHTDMABQ (5). The inset shows the molecular structure of PHTDMABQ.

III. RESULTS AND DISCUSSIONS

A. Electronic relaxation

Figure 1 shows the absorption and fluorescence spectra of a cast film sample of PHTDMABQ together with the output spectrum of the 6.3 fs NOPA laser used as pump and probe pulses. The molecular structure of PHTDMABQ is also shown in the inset of Fig. 1. Figure 2(a) shows the change in the absorbance as a function of pump-probe delay time at nine different probe photon energies.

Figure 3(a) shows the display of absorbance change plotted two-dimensionally against the probe delay time and probe photon energy. The following two decay features can be seen from the traces [Fig. 2(a)] and the two-dimensional plot (Fig. 3): (1) up to the probe delay time of 200 fs, the signal rapidly decays and then slowly decays up to 1.8 ps, which is the longest delay time in the present experiment. (2) During the first 100 fs, a spectral redshift is observed in the bleaching spectral range from 2.21 eV (560 nm) to 1.73 eV (716 nm).

The absorbance change $\Delta A(t,\omega)$ as functions of probe delay time (t) and probe frequency (ω) plotted in Fig. 2(a) was fitted with signal amplitude parameters of $a(\omega)$, $b(\omega)$, and $c(\omega)$ and time constants of τ_1, τ_2, and τ_3 in the following equation:

$$\Delta A(t,\omega) = a(\omega)e^{-t/\tau_1} + b(\omega)e^{-t/\tau_2} + c(\omega)e^{-t/\tau_3}. \quad (1)$$

The time-resolved spectra probed from 100 to 1700 fs with a 200 fs integration time width have a broad band with a negative ΔA peak at around 2.3 eV (540 nm), as shown in Fig. 3(b). The width was defined as the photon energy difference between 2.34 eV and that with the same ΔA value in the photon energy range of ~2.25 eV. The probe delay time dependence of the negative peak and the width together with their FT power spectra are plotted in Fig. 4, and both Figs. 4(a) and 4(c) were obtained with a time step of 1 fs. In Table I, we summarized the frequencies of the Fourier power spectra of real-time spectra [Fig. 2(b)], tracking the trace of a negative peak near 2.3 eV [Fig. 4(b)] and a width trace of the negative peak [Fig. 4(d)]. As shown in Table I, all of the frequencies of 1111, 1188, 1343, 1465, and 1583 cm^{-1} could be found either in Fig. 4(b) or in Fig. 4(d), or in both. This means that the 1111 cm^{-1} modulation frequency of the difference absorption spectra is due to the Herzberg-Teller-type spectral broadening,[26] and the modulation frequency of 1465 cm^{-1} is caused by the Franck-Condon-type wave packet motion.[27] The other absorbance modulations (1188, 1343, and 1583 cm^{-1}) of difference absorbance due to molecular vibration are induced by both the Franck-Condon-type and the Herzberg-Teller-type mechanisms.

In the photon energy range (wavelength) from 2.138 eV (580 nm) to 1.968 eV (630 nm), real-time traces can be fitted with Eq. (1) by a global fitting with the temporal parameters of $\tau_1 = 62 \pm 2$ fs, $\tau_2 = 750 \pm 20$ fs, and $\tau_3 \gg 3$ ps for "components" and with "spectra" of $a(\omega)$, $b(\omega)$, and $c(\omega)$ in Fig. 5, respectively. These results are useful to get insight into the spectral and temporal features of the system.

Here, let us discuss the features of the spectra $a(\omega)$, $b(\omega)$, and $c(\omega)$. Spectrum $a(\omega)$ has a positive-directed peak at around 2.02 eV (614 nm). This is due to the induced absorption, which competes with the stimulated emission, giving a broad negative signal. The stimulated emission spectrum was obtained from the observed spontaneous fluorescence spectrum, as shown in Fig. 1. The sharp slope in the spectral range of 2.08–2.13 eV (596–582 nm) is considered not to be due to a bleaching of the ground state absorption but due to the induced absorption, since the slope is opposite to that of a stimulated emission spectrum. The spectra $b(\omega)$ and $c(\omega)$ are both featureless and resemble each other, except for the difference in their slopes. The slope of $b(\omega)$ in the probed spectral range of 1.97–2.13 eV (630–580 nm) is less steep than that of $c(\omega)$ if the spectrum is normalized to each other. The slope of the bleaching spectrum is expected to be less steeper than the two time-resolved spectra of $b(\omega)$ and $c(\omega)$ if there is no other effect in the range. This, together with the dynamics of the $a(\omega)$, $b(\omega)$, and $c(\omega)$ components, will be discussed in the following.

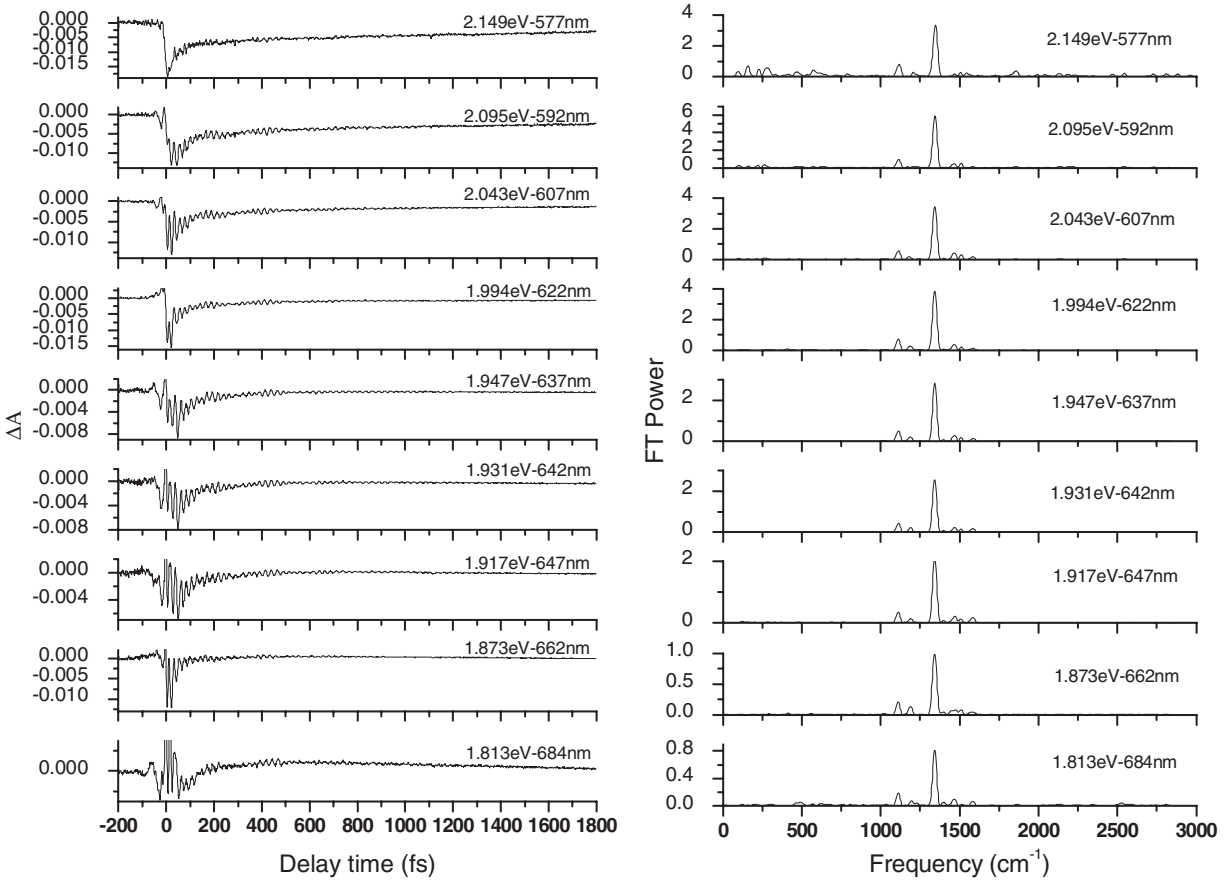

FIG. 2. (a) The changes in the absorbance as functions of pump-probe delay time at nine probe photon energies (wavelengths) and (b) the FT power spectra of real-time vibrational spectra at the corresponding probe energies.

By taking the spectral features and values of the time constants mentioned above into account, the following three possible mechanisms were proposed. In the schemes, the three time constants τ_1, τ_2, and τ_3 determined above can correspond to the processes in the following three sets of relaxation dynamics:

$$(1)\ S_n^{FC} \xrightarrow{\tau_1} S_m \xrightarrow{\tau_2} S_1 \xrightarrow{\tau_3} S_0 \quad (\text{or } T_1),$$
$$(2)\ S_n^{FC} \xrightarrow{\tau_1} S_1^{nTh} \xrightarrow{\tau_2} S_1^{Th} \xrightarrow{\tau_3} S_0 \quad (\text{or } T_1),$$
$$(3)\ S_1^{FC} \xrightarrow{\tau_1} S_1^{GR} \xrightarrow{\tau_2} S_1^{Th} \xrightarrow{\tau_3} S_0 \quad (\text{or } T_1).$$

Case (1) describes an excitation starting from the Franck-Condon (FC) state in the nth excited state S_n^{FC} and relaxing to the lower excited S_m state ($m<n$), which has a relatively long life of 750 ± 20 fs, relaxing to the lowest excited state (S_1) with much longer life than a few picoseconds. Then S_1 relaxes to the ground state (S_0) or the triplet state (T_1) with a microsecond lifetime. Case (2) describes an excitation to the Franck-Condon state (S_n^{FC}) of a nonthermal nth excited state followed by the relaxation to the lowest nonthermal excited state S_1^{nTh} by internal conversion and then relaxation to the thermal state S_1^{Th} followed by a decay to the S_0 or T_1 state. Case (3) describes an excitation to the higher vibrational level of the lowest excited electronic state S_1 in the Franck-Condon state (S_1^{FC}) and then a relaxation to the geometrically relaxed state (S_1^{GR}), which is the exciton polaron or sometimes called self-trapped exciton or neutral bipolaron.

Case (1) is less likely since there seems to be no indication of two more electronic states in the absorption spectrum corresponding to the excitation probe laser spectrum. It is also because of the nonexisting fluorescence excited at wavelengths in the laser spectral range. It can be discussed in such a way that the fluorescence efficiency of more than 10^{-3} is expected to be observed with such a long lifetime as 750 fs from the natural life of a few nanoseconds estimated from the integrated extinction coefficient over the spectral band. It is also a little difficult to explain the spectral shapes of $b(\omega)$ and $c(\omega)$, which are attributed to different electronic states from S_1 and S_0, respectively, and are very similar to each other with only a small difference in their slopes.

In case (2), the spectral change in the thermalization process of $S_1^{nTh} \xrightarrow{\tau_2} S_1^{Th}$ is due to the change in the population distribution of vibrational levels. Hence, the numbers of the components of various vibrational modes and vibrational quantum numbers are expected to be large. Therefore, it is not possible for the time-resolved spectra to be described in a limited number of spectral components. Instead, the

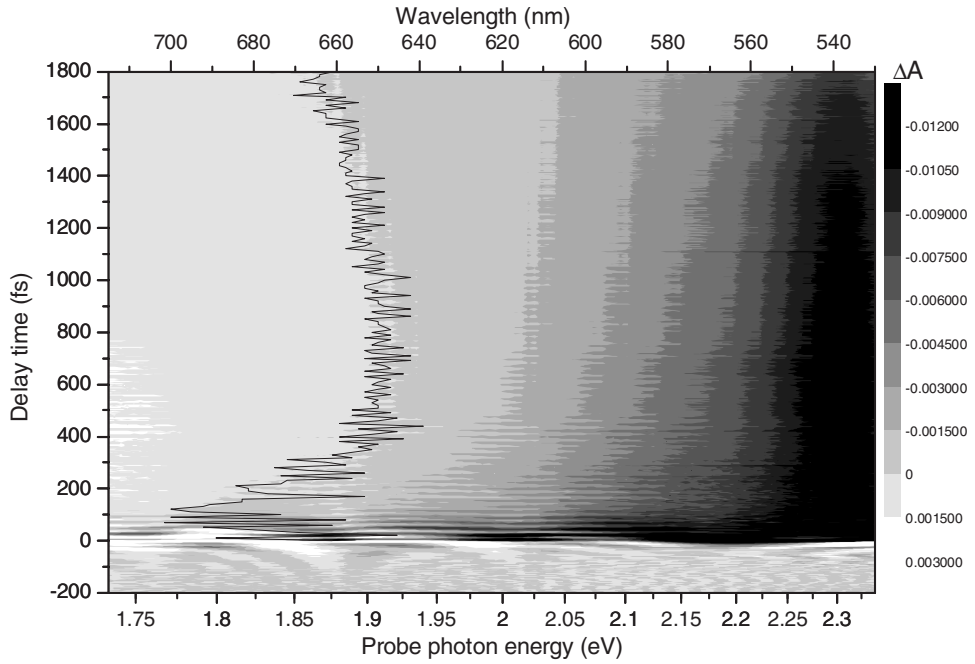

(a)

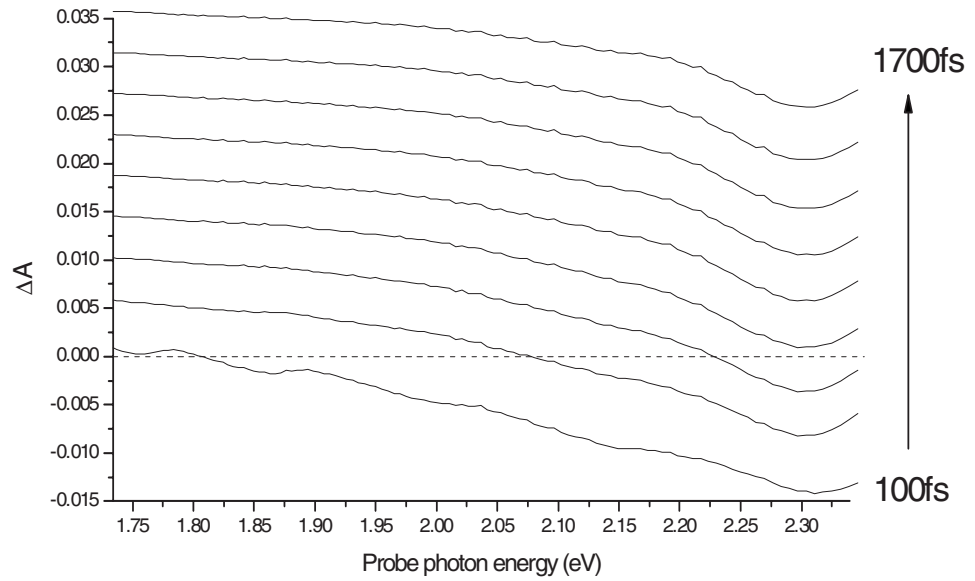

(b)

FIG. 3. (a) Two-dimensional display of the time dependence of the absorbance changes (probe photon energy versus probe delay time). The value of ΔA is shown by a pseudocolor, and the curve represents the probe photon energy where $\Delta A=0$. (b) The time-resolved pump-probe spectra (TRS) probed at nine center delay time points from 100 to 1700 fs with an integration time width of 200 fs. The spectral curves are shifted upward from TRS at 100 fs to 1700 fs with a step of 0.004.

changes in the spectral shapes in such cases are considered to be continuous. In such a case, there is no component with definite spectral shapes to be attributed to the intermediate species. Therefore, the time constants determined in Sec. II should simply be considered to be the average of distributed decay times. Since the decay functions are expected to be different at different wavelengths, it is also difficult to fit them with different analytic functions from exponential. Sometimes stretched exponential or power-law functions are used, and we tried to fit the result by these functions, but they did not fit well in the present case.

Even admitting the above mentioned ambiguity of the time constant, case (2) may be discussed as more likely because a thermalization time of 750 fs is reasonable in a polymer system. This may be reasonably explained in the following way. As in the case of polydiacetylenes, intrachain thermalization may take place in several hundred femtoseconds, and interchain thermalization takes place in 4–10 ps, which may correspond to $\tau_3 > 3$ ps in the present system.[9,15,16]

The small spectral difference between $b(\omega)$ and $c(\omega)$ is also reasonable in case (2). The energy distribution induced

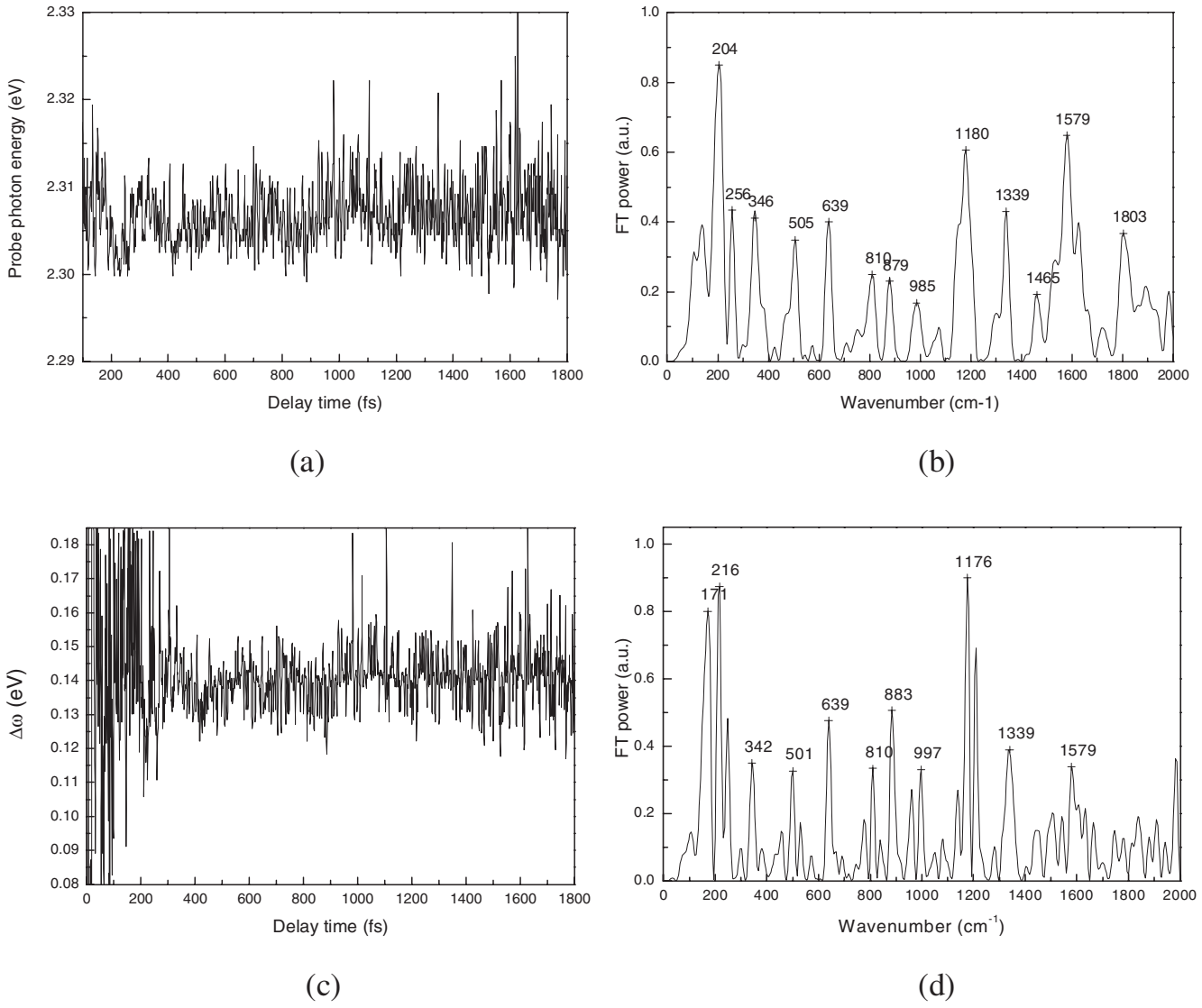

FIG. 4. (a) The probe delay time dependence of the negative peak tracking and (c) the width of graphs at around 2.3 eV shown in Fig. 3(b), and [(b) and (d)] their corresponding FT power spectra.

by the pump probe over several vibrational quantum numbers of relevant modes strongly coupled to the excitation electronic transitions has a distribution of 0.5 eV corresponding to about 4000 cm^{-1}. This width is much broader than the distribution range of molecular vibrations at an experimental temperature of about 293 K corresponding to 203 cm^{-1}. Hence, the thermalization process changes the population distribution of vibrational levels to be narrower by changing from a non-Boltzmann-type to a Boltzmann-type distribution.

Case (3) is discussed as even more likely. It is because the laser spectrum covers the higher vibrational levels of the lowest excited singlet state S_1. Also, the time constant of 62 fs is consistent with the self-trapping time, which was determined to be shorter than 100 fs for the free exciton to form an exciton polaron in polydiacetylene.[9] It is also close to the

TABLE I. Summary of frequencies appearing in Figs. 2(b), 4(b), and 4(d).

FT of real-time spectra (cm^{-1})	FT of negative peak tracking trace (cm^{-1})	FT of trace of negative peak width (cm^{-1})
1111		997
1188	1180	1176
1343	1339	1339
1465	1465	
1583	1579	1579

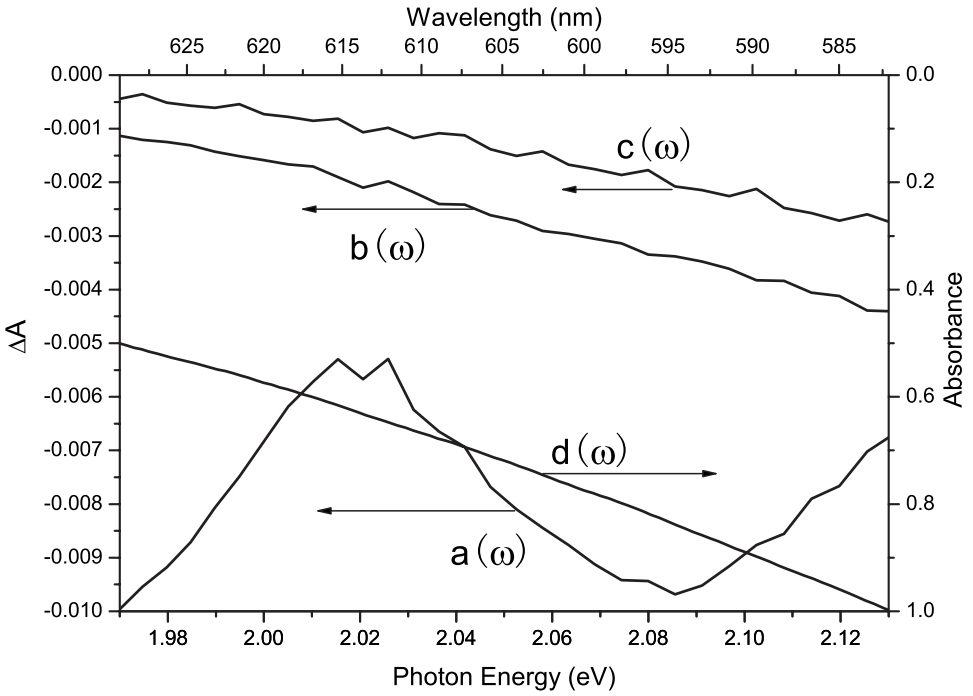

FIG. 5. The "spectra" of $a(\omega)$, $b(\omega)$, and $c(\omega)$ obtained by the global fitting, and $d(\omega)$ is the absorption spectrum.

decay time, which was determined to be about 50 fs for the breather mode to be converted to a soliton in *trans*-polyacetylene.[28] This model is discussed to be most reasonable in Sec. III B. A discussion of $S_1^{Th} \xrightarrow{\tau_3} S_0$ (or T_1) can be made in the same way as in case (2). We have concluded that case (3) is the electronic relaxation mechanism and we will discuss vibrational dynamics by using this model. The vibrational relaxation process is also found to be consistent with case (3).

B. Vibrational dynamics

Even with the accumulated information of the mechanism of electronic relaxations in conjugated polymers, their oligomers, and component monomer molecules, in many cases, it is still difficult to conclusively identify the relaxation mechanism and scheme. Recently, novel analysis methods such as singular value decomposition and/or global fitting have been developed, but it is still not easy to disentangle the relaxation dynamics in such a complicated system as amorphous conjugated polymers. It is because they are highly inhomogeneous in their electronic states and decay dynamics as previously mentioned.

Therefore, it is desirable to get more information than the data of electronic decay. For this purpose, we utilized the real-time vibrational spectroscopy to obtain both electronic and vibrational dynamics of the same system under the same excitation and probing condition by using the same sample and observing an amorphous phase, in which there is a relatively broad distribution of chain length, conjugation length, and degree of interaction strength between neighboring chains at the same time. Because of these requirements, the condition satisfied as mentioned above is considered to be most powerful to study such systems as conjugated polymers. The extension of this method to even more complicated systems such as a biological system is highly promising.

To identify the relaxation mechanism and discuss the vibrational dynamics during the relaxation processes, the probe wavelength of the Fourier powers of molecular modes coupled to the probed electronic transition was calculated. This FT analysis was performed after averaging over 200 fs to remove the slow decay dynamics due to dynamics in the relevant electronic states. The results are shown in Figs. 6 and 2(b). There are three prominent peaks at 1111, 1343, and 1465 cm^{-1}. The most intense peak located at 1343 cm^{-1} corresponds to the C-C stretching mode and it has a full width at half maximum (FWHM) of ~32.3 cm^{-1}, which corresponds to the vibrational dephasing time of ~361 fs. The dephasing time of the other two modes are also close to that of 1343 cm^{-1}, as shown in Table II. All of them have very short lifetimes of around 350–400 fs, which are much shorter than those of various vibrational modes in the ground state. This is because the modes belong to the electronic excited state. As we will discuss later, the peak of 1343 cm^{-1} is considered to result from the mixing of 1300 and 1350 cm^{-1} modes in the spectrogram calculation because of the finite frequency resolution in the numerical procedure set by the gate-time width.

In order to utilize the real-time trace in the vibrational dynamics study, which is considered to be useful for the identification of the mechanism, we calculated the spectrograms at 2.11 eV (586.6 nm), 2.06 eV (602.5 nm), and 2.01 eV (618.4 nm). A Blackman window of 120 fs half width at half maximum (HWHM) was used. The results are shown in Figs. 7(a)–7(c) and all of them show similar features.

The dynamics of the frequency components of 1300 and 1350 cm^{-1} was studied by taking the integrated amplitude of the corresponding components with a 20 cm^{-1} frequency width at each probe delay time. The components of 1300 and 1350 cm^{-1} have decay time of about 160 and 450 fs, respec-

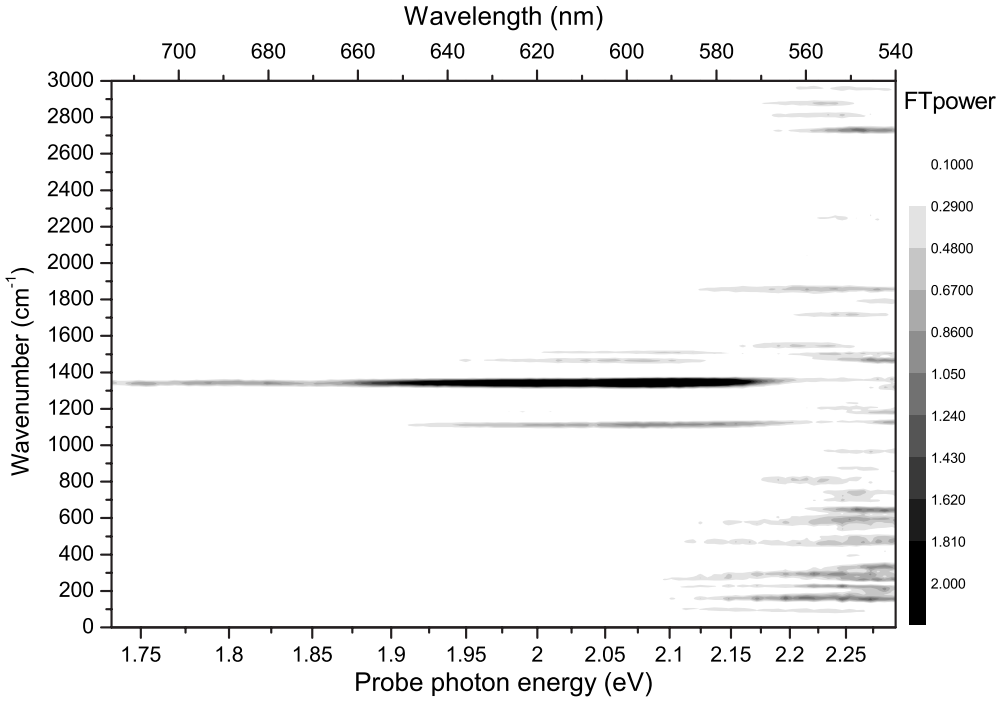

FIG. 6. FT power spectra of the pump-probe signal over the probe photon energy.

tively. The 1350 cm^{-1} component has the growth trace of about 100 fs. This frequency shift may be explained in terms of the change in the frequency from S_n^{FC} to S_m [case (1)], from S_n^{FC} to S_1^{nTh} [case (2)], and from S_1^{FC} to S_1^{GR} [case (3)]. The model of case (3) can even better explain the experimental results of the vibrational dynamics, which will be discussed in the following. The former decay time constant of 160 fs is overestimated because of the Blackman window of 120 fs HWHM. Therefore, it is reasonable to assume that the observed 160 fs corresponds to $\tau_1=62$ fs. Then this may indicate that the free exciton has an absorption feature of $a(\omega)$ and a vibrational frequency of 1300 cm^{-1}. It decays into the nonthermal exciton polaron with an electronic spectral feature of $b(\omega)$ that has a vibrational mode of 1350 cm^{-1} with $\tau_1=60\sim100$ fs. The mode frequencies of 1300 and 1350 cm^{-1} are considered to be C-C bond stretching in the free exciton and exciton polaron, respectively. The frequency of C-C bond increased after the geometrical relaxation because the strengthening of the lower frequency C-C bond takes place in the expense of the bond order in the higher frequency C-C bond in the thiophene ring associated with the formation of the exciton polaron.

Here, we would like to pay attention to the time dependency of the mode near 1500 cm^{-1}, which is due to one of the C-C stretching modes. At 150 fs, the peak frequency is downshifted to ~1445 cm^{-1} with the delay of 300 fs in accordance with the change of another C-C stretching mode with a lower frequency from 1300 to 1350 cm^{-1} in the same time range. The frequency difference in both cases is similar (about 50 cm^{-1}). Therefore, it can be considered that the vibrational energy of the lower frequency mode due to the smaller bond order is increased at the expense of the higher frequency C-C stretching frequency by a similar amount of 50 cm^{-1}. These frequency changes are due to the more uniform π-electron distribution in the exciton polaron state. Further, to obtain a more reliable identification of the state, we studied the vibrational phase of the modes at 1300 cm^{-1} in the 50–220 fs delay time range and that of 1350 cm^{-1} in 300–700 fs. The coherent molecular vibration after the geometrical relaxation is considered to be a kind of reaction induced coherence. This coherent vibration decays with the time constant of about 450 fs.[29–31]

TABLE II. Bandwidths and corresponding dephasing times of the three modes.

Wavenumber (cm^{-1})	FWHM (cm^{-1})	Dephasing time (fs)
1111	29.6	394
1343	32.3	361
1465	29.8	391

In conclusion, we utilized the real-time vibrational spectroscopy to obtain both electronic and vibrational dynamics of the same system under the same excitation and probing condition and observed an amorphous phase, in which there is a relatively broad distribution of chain length, conjugation length, and degree of interaction strength between neighboring chains at the same time. Because of these requirements, the condition satisfied, as mentioned above, is considered to be the most powerful to study such systems as conjugated polymers. By using this method, we could observe the spectral change in the electronic absorption spectrum and instantaneous vibrational frequency and could clarify the mechanism of the ultrafast geometrical relaxation in a conjugated polymer. In the polymer PHTDMABQ, the geometrical relaxation from the free exciton to the exciton polaron takes place in 60–100 fs. This time is close to that observed in

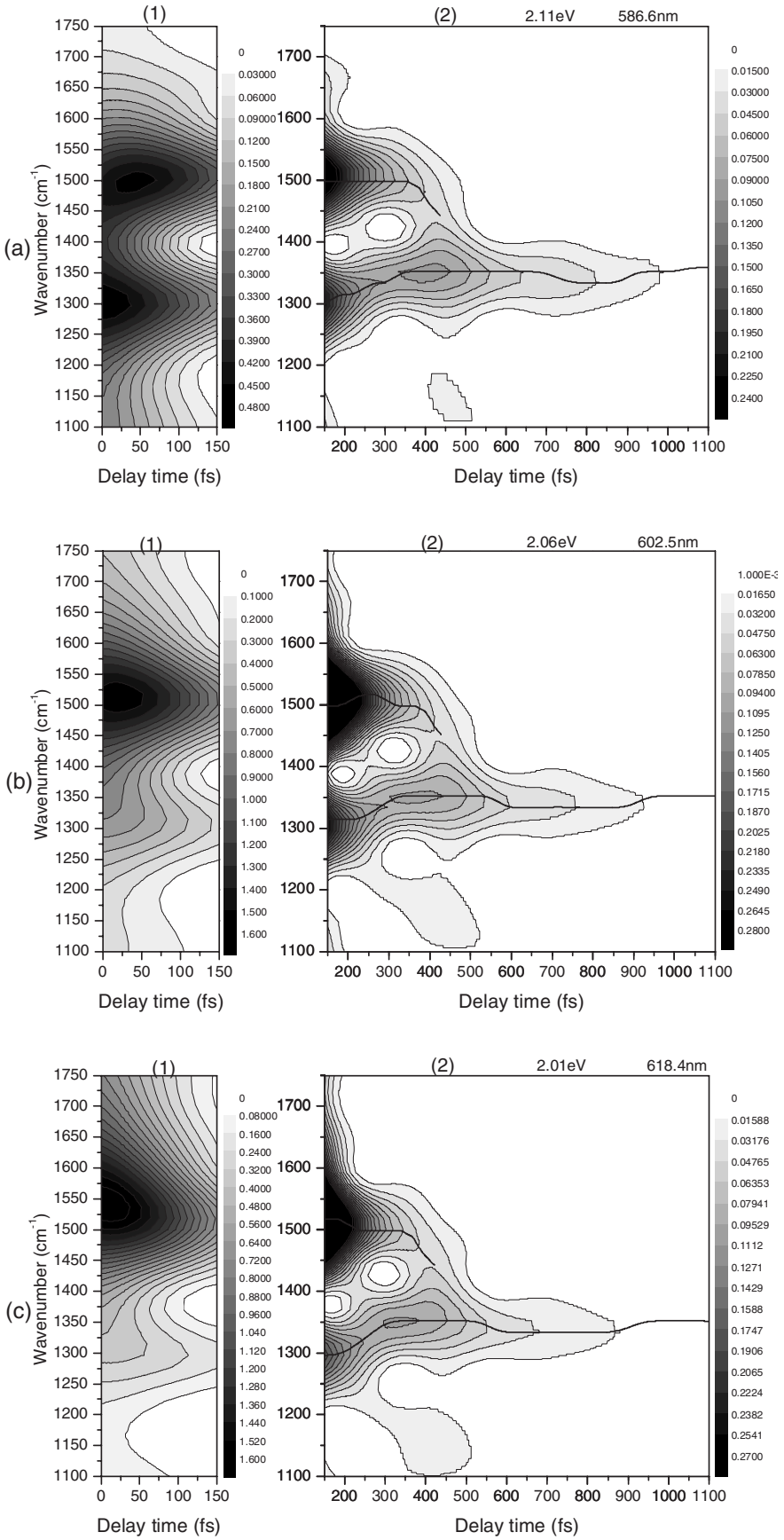

FIG. 7. Contour maps of the two-dimensional Fourier power of vibrational components obtained by spectrogram calculation for the real-time data calculated at (a) 2.11 eV, (b) 2.06 eV, and (c) 2.01 eV. The solid lines denote peak frequency modulations.

several polydiacetylenes. The C-C bond stretching frequencies of the free exciton and exciton polaron are 1300 and 1350 cm^{-1}. The coherent molecular vibration after the geometrical relaxation is considered to be a kind of reaction induced coherence. This coherent vibration decays with the time constant of about 450 fs. The extension of this method of simultaneous measurement of electronic and vibrational dynamics to even more complicated systems such as a biological system is highly desired.

ACKNOWLEDGMENTS

This work was partly supported by a grant from the Ministry of Education (MOE) in Taiwan under the ATU Program at National Chiao Tung University. A part of this work was performed under the Joint Research Project of the Institute of Laser Engineering, Osaka University, under Contract No. B1-27.

*kobayashi@ils.uec.ac.jp

[1] L. J. Rothberg and A. J. Lovinger, J. Mater. Res. **11**, 3174 (1996).
[2] F. Hide M. A. DÍaz-GarcÍa, B. J. Schwartz, and A. J. Heeger, Acc. Chem. Res. **30**, 430 (1997).
[3] R. H. Friend, R. W. Gymer, A. B. Holmes, J. H. Burroughes, R. N. Marks, C. Taliani, D. D. C. Bradley, D. A. Dos Santos, J. L. Brédas, M. Lögdlund, and W. R. Salaneck, Nature (London) **397**, 121 (1999).
[4] G. A. M. Sáfar, F. A. C. Oliveira, L. A. Cury, A. Righi, P. L. M. Barbosa, P. Dieudonné, and F. S. Lameiras, J. Appl. Polym. Sci. **102**, 5620 (2006).
[5] T. Kobayashi, *Nonlinear Optics of Organics and Semiconductors* (Springer, Berlin, 1989).
[6] A. J. Heeger, S. Kivelson, J. R. Schrieffer, and W.-P. Su, Rev. Mod. Phys. **60**, 781 (1988).
[7] S. Etemad and Z. G. Soos, in *Spectroscopy of Advanced Materials*, edited by R. J. H. Clark and R. E. Hester (Wiley, New York, 1991).
[8] R. F. Mahrt, T. Pauck, U. Lemmer, U. Siegner, M. Hopmeier, R. Hennig, H. Bässler, E. O. Göbel, P. Haring Bolivar, G. Wegmann, H. Kurz, U. Scherf, and K. Müllen, Phys. Rev. B **54**, 1759 (1996).
[9] T. Kobayashi, M. Yoshizawa, U. Stamm, M. Taiji, and M. Hasegawa, J. Opt. Soc. Am. B **7**, 1558 (1990).
[10] E. I. Rashba, in *Excitons*, edited by E. I. Rashba and M. D. Struge (North-Holland, Amsterdam, 1987), p. 273.
[11] G. Wegner, Makromol. Chem. **145**, 85 (1971).
[12] G. N. Patel, R. R. Chance, and J. D. Witt, J. Chem. Phys. **70**, 4387 (1979).
[13] D. Bloor, in *Polydiacetylenes*, edited by D. Bloor and R. R. Chance (Nijhoff, Dordrecht, 1985).
[14] K. Tashiro, K. Ono, Y. Minagawa, M. Kobayashi, T. Kawai, and K. Yoshino J. Polym. Sci., Part B: Polym. Phys. **29**, 1223 (1991).
[15] M. Yoshizawa, T. Kobayashi, H. Fujimoto, and J. Tanaka, J. Phys. Soc. Jpn. **56**, 768 (1987).
[16] M. Yoshizawa, K. Nishiyama, and T. Kobayashi, Chem. Phys. Lett. **207**, 461 (1993).
[17] *Time-Resolved Vibrational Spectroscopy*, Springer Proceedings in Physics Vol. 4, edited by A. Laubereau and M. Stockburger (Springer-Verlag, Berlin, 1985).
[18] *Time-Resolved Vibrational Spectroscopy V*, Springer Proceedings in Physics Vol. 68, edited by H. Takahashi (Springer-Verlag, Berlin, 1991).
[19] *Time-Resolved Vibrational Spectroscopy VI*, Springer Proceedings in Physics Vol. 74, edited by A. Lau, F. Siebert, and W. Werncke (Springer-Verlag, Berlin, 1993).
[20] A. Shirakawa and T. Kobayashi, Appl. Phys. Lett. **72**, 147 (1998); IEICE Trans. Electron. **81-C**, 246 (1998).
[21] T. Wilhelm, J. Piel, and E. Riedle, Opt. Lett. **22**, 1494 (1997).
[22] G. Cerullo, M. Nisoli, and S. De Silvestri, Appl. Phys. Lett. **71**, 3616 (1997); Opt. Lett. **23**, 1283 (1998).
[23] A. Shirakawa, I. Sakane, and T. Kobayashi, Opt. Lett. **23**, 1292 (1998).
[24] A. Baltuška, T. Fuji, and T. Kobayashi, Opt. Lett. **27**, 306 (2002).
[25] A. Shirakawa, I. Sakane, and T. Kobayashi, in *Ultrafast Phenomena XI*, edited by T. Elsaesser, J. G. Fujimoto, D. A. Wiersma, and W. Zinth (Springer-Verlag, Berlin, 1998), p. 54; A. Shirakawa, I. Sakane, M. Takasaka, and T. Kobayashi, Appl. Phys. Lett. **74**, 2268 (1999).
[26] H. Kano, T. Saito, and T. Kobayashi, J. Phys. Chem. A **106**, 3445 (2002).
[27] T. Kobayashi, Z. Wang, and T. Otsubo, J. Phys. Chem. A **111**, 12985 (2007).
[28] S. Adachi, V. M. Kobryanskii, and T. Kobayashi, Phys. Rev. Lett. **89**, 027401 (2002).
[29] L. Zhu, A. Widom, and P. M. Champion, J. Chem. Phys. **107**, 2859 (1997).
[30] F. Rosca, A. T. N. Kumar, X. Ye, T. Sjodin, A. A. Demidov, and P. M. Champion, J. Phys. Chem. A **104**, 4280 (2000).
[31] F. Rosca, A. T. N. Kumar, D. Lonascu, T. Sjodin, A. A. Demidov, and P. M. Champion, J. Chem. Phys. **114**, 10884 (2001).